Eur Biophys J (2008) 37:393–402
DOI 10.1007/s00249-007-0224-5

ORIGINAL PAPER

Modeling study of mecamylamine block of muscle type acetylcholine receptors

Konstantin Ostroumov · Asya Shaikhutdinova · Andrey Skorinkin

Received: 16 August 2007 / Revised: 18 September 2007 / Accepted: 21 September 2007 / Published online: 16 October 2007

Abstract The blocking action of mecamylamine on different types of nicotinic acetylcholine receptors (nAChRs) has been extensively studied and used as a tool to characterize the nAChRs from different synapses. However, mechanism of mecamylamine action was not fully explored for all types of nAChRs. In the present study, we provide brief description of the mecamylamine action on muscle nAChRs expressed at the frog neuromuscular junction. In this preparation mecamylamine block of nAChRs was accompanied by a use-dependent block relief induced by membrane depolarization combined with the activation of nAChRs by endogenous agonist acetylcholine (ACh). Further, three kinetic models of possible mecamylamine interaction with nAChRs were analyzed including simple open channel block, symmetrical trapping block and asymmetrical trapping block. This analysis suggested that mecamylamine action could be described on the basis of trapping mechanism, when the antagonist remained inside the channel even in the absence of bound agonist. Such receptors with trapped mecamylamine inside were predicted to have a closing rate constant about three times faster than resting one and a fast voltage-dependent unblocking rate constant. Specific experimental conditions and morphological organization of the neuromuscular synapses were considered to simulate time course of the mecamylamine block development. Thus, likewise for the neuronal nAChRs, the trapping mechanism determined the action of mecamylamine on synaptic neuromuscular currents evoked by the endogenous agonist acetylcholine (ACh), however specific morphological organization of the synaptic transmission delayed time development of the currents block.

Keywords Muscular nicotinic acetylcholine receptors · Trapping block · Mecamylamine · Mathematical modeling · Zonal organization of transmitter release

K. Ostroumov (✉)
Neurobiology Sector and S.P.I.N.A.L. Project,
International School for Advanced Studies (SISSA),
Area Science Park, Q1 Building, Strada Statale 14,
34012 Basovizza, Trieste, Italy
e-mail: konstantin.ostroumov@medisin.uio.no

A. Shaikhutdinova
Kazan Institute of Biochemistry and Biophysics RAS,
Lobachevskogo 2, 420008 Kazan, Russia

A. Skorinkin
Kazan State University, Kremlevskaya 18,
420008 Kazan, Russia

A. Skorinkin
Russia and Kazan Institute of Biochemistry and Biophysics
RAS, Lobachevskogo 2, 420008 Kazan, Russia

Present Address:
K. Ostroumov
Department of Physiology, IMB, and Centre
for Molecular Biology and Neuroscience,
University of Oslo, Domus Medica: room 1131,
Sognvannsveien 9, Gaustad, PB 1104 Blindern,
N0317 Oslo, Norway

Introduction

Nicotinic acetylcholine receptors (nAChRs) are blocked by noncompetitive inhibitors interacting with the receptor complex at distinct sites along the ionic channel (for review see Corringer et al. 2000). In general, noncompetitive inhibitors are divided into blockers which interact with

closed or open channels, or agents trapped by channel closure after binding inside the open channel (Benveniste and Mayer 1995; Dingledine et al. 1999; Gurney and Rang 1984). The latter case, so-called trapping mechanism, was largely studied regarding glutamate receptors (Blanpied et al. 1997; Chen and Lipton 1997; Dorrscheidt-Kafer 1981; Vargas-Caballero and Robinson 2004), and might be observed at cholinergic receptors as well (Giniatullin et al. 2000; Lingle 1983a, b; Neely and Lingle 1986).

In the early studies it has been found that mecamylamine blocks muscle nAChRs in a use- and voltage-dependent manner (Albuquerque et al. 1985; Blackman and Ray 1964; Varanda et al. 1985). These authors have considered the simple open channel block mechanism of mecamylamine interaction with nAChRs, but noted that mecamylamine block cannot be fully described by a simple open-channel blocking scheme with only one blocked state. Moreover, studies on the model of rat chromaffin cells explored more sophisticated mechanism of mecamylamine action. It was shown that mecamylamine blocks the nicotinic currents via trapping mechanism (Giniatullin et al. 2000). The main feature of this block is the phenomenon of block relief, which might be revealed by combined action of depolarization and activation of nAChRs. Our previous experimental study (Skorinkin et al. 2004) of the mecamylamine action on muscle nAChRs revealed that: (1) mecamylamine (1–20 μM) reduced evoked end-plate currents (EPC) amplitude with Hill's constant equal to 1.2 and IC_{50} = 7.8 μM at holding potential –70 mV; (2) the calculated depth of its interaction with the muscle nAChR channel was almost half of the one of neuronal nAChRs (0.37 compare to 0.72 for neuronal nAChRs); (3) simultaneous membrane depolarization and repetitive activation of postsynaptic nAChRs by motor nerve stimulation produced rapid block relief dependent on the degree of depolarization, number of conditioning signals and mecamylamine concentration, and only slightly depended on the rate of stimulation.

Specifically, mecamylamine at 20 μM concentration decreased the amplitude of multiquantal end-plate currents (EPCs) elicited every 20 s (recorded at –70 mV holding potential) to 28 ± 2% of control (n = 8; $P < 0.05$), an effect reaching steady state after 25–30 min. Shortening of EPC decay time constant (τ) to 57 ± 4% of control accompanied the depression of EPCs amplitude.

In standard conditions the voltage dependence of EPC peak amplitude was linear in the range from 0 to –100 mV, indicating efficient voltage control. Consistent with classical properties of open channel block (Albuquerque et al. 1985) there was strong non-linearity of the *I/V* plots indicating that the mecamylamine block was stronger at –100 mV than at –20 mV for either concentration tested. The EPC depression in the presence of 20 μM mecamylamine was so strong that the EPC peak amplitude became little sensitive to the holding potential. The EPC decay time constant also became virtually insensitive to potential and was largely decreased particularly by 20 μM mecamylamine. However, in the presence of 5 μM mecamylamine, EPC amplitude and τ_{EPC} at –20 mV did not differ from control. These findings suggest that mecamylamine blocked nAChRs in a voltage- and concentration-dependent manner.

We report here that the trapping mechanism is applicable to the action of mecamylamine on the full-quantal content synaptic currents evoked by the endogenous agonist acetylcholine (ACh). Modeling results indicated that retarded isomerization of trapped receptors from closed blocked state into open one provided one possible mechanism for slow dynamics of nAChRs in the presence of mecamylamine. Moreover, zonal organization of the synaptic release, ACh concentration profile inside the synaptic cleft and perfusion rate were considered to simulate delayed development of mecamylamine effects.

Methods

Experimental procedures

Experimental procedures and main experimental results were described in our previous paper (Skorinkin et al. 2004) and above in the Introduction. Briefly, experiments were performed on an in vitro sartorius neuro-muscular preparation from the frog *Rana Ridibunda* at room temperature. The experiments were conducted according to the principles and requirements of the European Communities Council Directive (24 November 1986; 86/609/EEC). Muscles with attached nerves were dissected free, placed in a recording chamber, and continuously perfused with Ringer solution (see Skorinkin et al. 2004 for details about preparation and solutions). Muscle contractions were then eliminated by transverse cutting of muscle fibres. Cut muscle was rinsed for at least 40 min and fixed to the Sylgard bottom of the recording chamber.

Recording of synaptic currents was performed using the standard two-electrode voltage clamp technique. Endplates from fine intramuscular nerve branches were localized visually. End-plate currents (EPCs) were elicited by supramaximal nerve stimulation with different inter-stimulation intervals (see Results). Intracellular electrodes filled with 2.5 M KCl had 3–5 MΩ resistance. During current recording, holding potential was maintained at –70 mV (unless otherwise indicated). If injected current became more than 100 nA, data were discarded. Recorded EPCs were digitized at 50 kHz and stored on a hard-disk.

Computer simulation method

The nicotinic receptor current ($I_{(t)}$) at a given time (t) was calculated according to:

$$I(t) = V \cdot N \cdot P_{\text{open}}(t) \cdot \sigma, \quad (1)$$

where V is the test voltage (mV), N number of nicotinic channels, P_{open} probability of open channel state, and σ is the channel conductance (we assumed σ to be constant).

For each receptor kinetic scheme, based on the mass action law, we formulated a set of differential equations in analogy with the approach used by Chretien and Chauvet (1998), whereby:

$$\frac{d\bar{P}(t)}{dt} = \bar{P}(t) \cdot Q, \quad (2)$$

where $\bar{P}$ is a vector composed of the receptor probabilities to occupy each kinetic state at time t, and Q is the matrix of transitions between the states.

The voltage dependence (H_i) of rate constant k_i governing the transition of receptors between distinct kinetics states was obtained from:

$$k_i(V) = k_i(0\text{mV}) \cdot e^{\frac{V}{H_i}}, \quad (3)$$

where V is the test voltage (mV) (Maconochie and Knight 1992; Mathie et al. 1990).

The ACh concentration in the synaptic cleft was described using the following equation:

$$\frac{d\,[A]}{dt} = w(t) - u \cdot [A] - f(t) \cdot [A] + k_1^- \cdot [AR] + k_2^- \cdot [A_2R] - k_1^+ \cdot [A] \cdot [R] - k_2^+ \cdot [A] \cdot [AR] \quad (4)$$

where $[A]$ is the ACh concentration, presynaptic agonist release is denoted as $w(t)$[mM/l ms], coefficient u describes cleft diffusion and uptake (120 ms^{-1}), $f(t)$ is the rate of ACh degradation [1/m]. Previous analysis (Skorinkin and Shaikhutdinova 2004) allowed to determine $w(t)$ and $f(t)$ for the frog neuromuscular junction:

$$w(t) = 3,200 \cdot \left(1 - e^{-\frac{t}{0.4}}\right) \cdot e^{-\frac{t}{0.035}} + 174 \cdot \left(1 - e^{-\frac{t}{0.165}}\right) \cdot e^{-\frac{t}{0.385}},$$

and

$$f(t) = 207,000 \cdot \left(1 - e^{-\frac{t}{0.89}}\right)^9 \cdot e^{-\frac{t}{0.58}} + 1,240 \cdot \left(1 - e^{-\frac{t}{1.2}}\right)^{1.3}.$$

Equation (4) was added to each set of the differential equations (2) describing kinetic schemes under consideration.

Number of active ACh release zones (AZ) activated j times at ith successive stimulation (n_{ij}, where $j \le i$) was calculated using the following equation:

$$n_{i,j} = p \cdot n_{i-1,j-1} + (1 - p) \cdot n_{i-1,j}, \quad (5)$$

where p is the probability of release from each zone after single nerve stimulation, $n_{0,0} = 300$ and $n_{0,j} = 0$ for $j > 0$. In our calculations we used $p = 0.2$ obtained as a result of EPCs quantal content analysis (unpublished data).

The recorded EPCs were represented as a sum of local currents elicited at the postsynaptic membrane lying opposite to each AZ. Assuming that local currents parameters are the same for all zones activated equal number of times, we calculated the end-plate current parameters (D_i) for ith stimulation using the following equation:

$$D_i = \frac{\sum_{j=1}^{i} a_j \cdot n_{i,j}}{M}, \quad (6)$$

where a_j is a value of local current parameter under consideration, M is the total number of AZs.

The further model development required consideration of a relatively slow solution exchange rate in the recording chamber. In all experiments this rate was constant and equal to 0.35 ml/min. The solution exchange rate (q), constant bath volume (V) and drug concentration applied to the perfusion system (C_0) were used to calculate time profile of drug concentration in the chamber (C):

$$C = C_0 \cdot \left(1 - e^{\frac{-q}{2 \cdot V} \cdot t}\right). \quad (7)$$

During drug wash out its bath concentration degradation was described by the following equation:

$$C = C_1 \cdot e^{\frac{-q}{2 \cdot V} \cdot t}, \quad (8)$$

where C_1 is the established drug concentration.

Our in-house developed program was written in Pascal language and used on an IBM-compatible PC to solve numerically sets of differential equations (2) using the eight-order Runge–Kutta method (Baker et al. 1998).

Results

Computational modeling of nAChR kinetics in the presence of mecamylamine

The mechanism of mecamylamine block was investigated using computer-assisted simulation of multiquantal EPCs. We tested whether the experimental data could be adequately fitted by assuming either simple open channel

block by mecamylamine or a more complex process involving change in receptor kinetics.

A model was considered acceptable if it could fully satisfy the following criteria by reproducing: (1) the time course and degree of changes in EPC amplitude and decay time analogous to the one found experimentally with mecamylamine block (see Fig. 1Aa); (2) block relief after a depolarization step only in coincidence with nerve stimulation (Fig. 1Ab); (3) amplitude changes before, during and after membrane depolarization with the same time course observed experimentally at 10 Hz stimulation (Fig. 1Ac). In general, for modeling we assumed that kinetics of nAChR interaction with the agonist could be described by a simplified scheme (Colquhoun 1998):

$$R + A \underset{k_1^-}{\overset{k_1^+}{\leftrightarrow}} ARA \underset{k_2^-}{\overset{k_1^+}{\leftrightarrow}} A_2 R \underset{\alpha}{\overset{\beta}{\leftrightarrow}} A_2 R*,$$

where k_1^+, k_1^-, k_2^+, k_2^-, β and α are rate constants for agonist binding/unbinding and isomerization, A is an agonist, R and $R*$ represent the closed and open states of the channels, respectively. Note that although β has minimal voltage dependence, α has a moderate degree of voltage dependence (H = 126 mV; Magleby and Stevens 1972). To simplify our

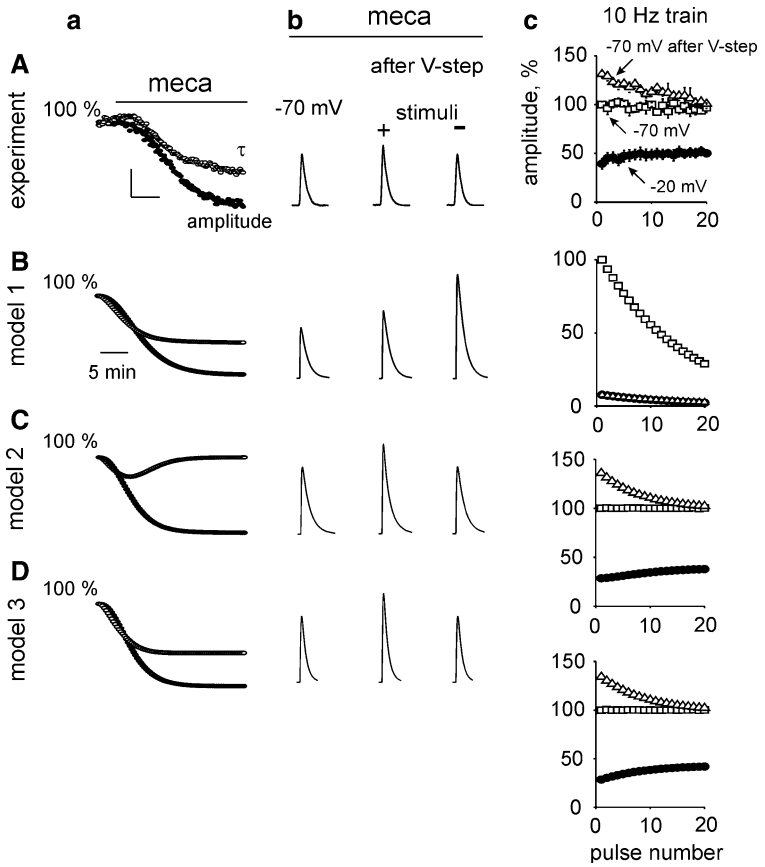

Fig. 1 Only the open channel block scheme with trapping mechanism could reproduce all experimental results. *Horizontally* organized panels marked with capital letters *A*, *B*, *C* and *D* show experimental results (experiment) and results obtained using simple channel block scheme (model 1), symmetrical trapping scheme (model 2) and asymmetrical trapping scheme (model 3), respectively. *Vertically* organized panels show results obtained during different experimental protocols: column (**a**) shows development of mecamylamine action on amplitude and decay time (τ) of evoked EPCs (% of control; averaged amplitude and τ in control stand for 100%; 0.05 Hz nerve stimulation); column (**b**) compares averaged EPCs at steady state mecamylamine block before and after depolarizing step to –20 mV (after V-step) accompanied by (stimuli +) or without (stimuli –) low frequency nerve stimulation (0.05 Hz); column (**c**) shows plots of peak amplitude of EPCs during high frequency stimulation (10 Hz train) before (*open square* –70 mV), during (*filled circle* –20 mV) and after (*open riangle* –70 mV after V-step) membrane depolarization to –20 mV versus nerve stimulus number in the train. *A***a** experimentally obtained data (τ, *open circles*, and amplitude, *filled circles*) during application of 20 μM mecamylamine are shown (*horizontal* and *vertical* bars stand for 10 min and 25% of EPC amplitude, respectively). Note that block relief (*A***b**) appears after membrane depolarization (after V-step) concurrent with low frequency nerve stimulation (stimuli +). *B* Simulated responses based on the simple channel block scheme. Time course of block development is reproduced (note, however, faster time scale; see Fig. 3b), but relief characteristics and stimulus dependence are not (*B***b**, *B***c**). *C* Symmetrical trapping scheme reproduces the main characteristics of mecamylamine block except the decay time constant changes during block development (*C***a**). *D* The asymmetrical trapping scheme provides a close replica of all the properties of mecamylamine action (*D***a**–*D***c**; compare with *A***a**–*A***c**)

Table 1 Kinetic values used for computer modeling of mecamylamine block of ACh-induced currents

	Simple open channel block	Symmetrical trapping scheme	Asymmetrical trapping scheme
k_1^+, $mM^{-1}\cdot ms^{-1}$	160	160	160
k_1^-, ms^{-1}	18	18	18
k_2^+, $mM^{-1}\cdot ms^{-1}$	80	80	80
k_2^-, ms^{-1}	36	36	36
β, ms^{-1}	36.7	36.7	36.7
α, ms^{-1} *	1.7	1.7	1.7
k_b^+, $mM^{-1}\cdot ms^{-1}$	32	260	300
k_b^-, ms^{-1}	0.000018 (H_d = 450 mV)	2.0 (H_d = 32 mV)	3.2 (H_d = 27.5 mV)
$k_1^{+\prime}$, $mM^{-1}\cdot ms^{-1}$	–	160	160
$k_1^{-\prime}$, ms^{-1}	–	18	18
$k_2^{+\prime}$, $mM^{-1}\cdot ms^{-1}$	–	80	80
$k_2^{-\prime}$, ms^{-1}	–	36	36
β', ms^{-1}	–	36.7	36.7
α', ms^{-1} *	–	1.7	4.5

*– For all cases the same degree of voltage dependence was assumed (H_α = 126 mV); the value in the Table 1 is for –70 mV

scheme, we assumed that there was no significant receptor desensitization (Giniatullin et al. 1989, 2005; Naves and van der Kloot 2001). Values for rate constants used during simulation were taken from previous experimental and modeling study of muscle nAChRs (Stiles et al. 1999) and shown in Table 1. While, Stiles et al. (1999) used lizard (*Anolis carolinensis*) intercostal muscle to determine rate constants, their results were successfully used to simulate EPCs recorded at frog neuromuscular junction (Pryaznikov et al. 2002, 2005; Skorinkin 2005; Skorinkin and Shaikhutdinova 2004). In general, it is accepted that there are just two types of muscle nAChRs (fetal and adult) and each type has the same subunit composition and similar time course of electrophysiological signals at frog and other neuromuscular junctions (Anglister et al. 1994; Brammar 1996; Kalamida et al. 2007; Stiles et al. 1999). Table 2 summarizes quantitative measurements of experimentally obtained characteristics. Three models were investigated.

Model 1: simple open channel block

Open channel block is the simplest model of antagonist interaction with the nAChR complex. The assumption that the mecamylamine action could be explained on the basis of this scheme was discussed by Shen and Horn (1998). Such interaction can be represented as the following:

$$R + A \underset{k_1^-}{\overset{k_1^+}{\leftrightarrow}} AR + A \underset{k_2^-}{\overset{k_2^+}{\leftrightarrow}} A_2R \underset{\alpha}{\overset{\beta}{\leftrightarrow}} A_2R* + B \underset{k_b^-}{\overset{k_b^+}{\leftrightarrow}} A_2RB,$$

where B is mecamylamine, k_b^+ and k_b^- is blocking and unblocking rate constant, respectively. Note that in this model only one blocked state of receptor exists. The rate constant k_b^- is responsible for unblocking of receptor and its value together with time interval between nerve stimuli determine the steady state level of EPCs.

Figure 1B and Table 2 show that this model could not fit experimental data fully. It predicts that block relief can be obtained just by a membrane depolarization (Fig. 1Bb) and it is even bigger without stimulation because the recovery in this scheme depends only from the time between stimulations. The isomerization rate constant α increases with membrane depolarization (Table 2) and longer time is necessary for receptor unblocking (compared to depolarization plus stimulation). Moreover, strong augmentation of use-dependent block by 10 Hz nerve stimulation occurred (Fig. 1Bc) and no block relief (during or after membrane depolarization) was observed (Table 2). Receptor block by more than one molecule of mecamylamine was discarded as a modification of simple open channel block when unblocking depends only on the receptor activation time.

Model 2: symmetrical trapping mechanism

Since simple open channel block failed to reproduce our experimental data we next considered a more complex scheme with antagonist trapping within the nAChR. This type of block is based on the assumption that the antagonist remains inside a closed channel (Gurney and Rang 1984;

Table 2 Comparison of experimentally obtained and simulation-based characteristics of 20 μM mecamylamine block

	Steady state peak current, % of control	Steady state τ, % of control	% Relief. no stimulation*	% Relief. 0.05 Hz stimulation*	% Relief. 10 Hz stimulation*
Experiment	28 ± 2	57 ± 4	1 ± 3	34 ± 5	31 ± 5
Model 1	28	58	**149**	31	**–99**
Model2	28	**100**	0	31	31
Model 3	29	57	0	32	31

* In all three cases the membrane was depolarized to –20 mV from holding potential of –70 mV for 2 min

Bold indicates modeling results inconsistent with experimentally obtained data

Lingle 1983b). To start with, we assumed the simplest case when the presence of antagonist inside the channel did not change the receptor kinetics. This means that all rate constants remained the same when the antagonist occupied the ionic pore (symmetrical trapping scheme). The scheme can be represented as following:

$$R + A \underset{k_1^-}{\overset{k_1^+}{\leftrightarrow}} AR + A \underset{k_2^-}{\overset{k_2^+}{\leftrightarrow}} A_2R \underset{\alpha}{\overset{\beta}{\leftrightarrow}} A_2R* + B$$

$$k_b^- \updownarrow k_b^+$$

$$RB + A \underset{k_1^{-\prime}}{\overset{k_1^{+\prime}}{\leftrightarrow}} ARB + A \underset{k_1^{-\prime}}{\overset{k_2^{+\prime}}{\leftrightarrow}} A_2RB \underset{\alpha'}{\overset{\beta'}{\leftrightarrow}} A_2R* B,$$

where A_2R^*B is still an open state of receptor but current does not pass through it because of the antagonist molecule presence; A_2RB, ARB and RB are receptor closed states with two, one or no bound agonist molecules, respectively, and one molecule of antagonist trapped inside the channel (see Table 1 for rate constants values). Results of our modeling study (Fig. 1C; Table 2) indicate that predicted changes in the EPC decay time constant do not follow the experimentally observed ones (compare Fig. 1Ca with Aa). However, this model can replicate many other features of the action of mecamylamine including block relief (see Fig. 1Ca–Cc; Table 2), suggesting that this scheme might be used for further analysis, but it required refinement.

Model 3: asymmetrical trapping mechanism

Following the previous studies of antagonist trapping mechanism (Dilmore and Johnson 1998; Giniatullin et al. 2000), we assumed that presence of the antagonist molecule inside the channel could change kinetics of channel opening and closing. Such a scheme is the same as for the Model 2 with the certain modifications in rate constants (see Table 1). The average transitions between A_2R^* and A_2R^*B are assumed to be zero to ensure identical amplitude at steady state block, so the equilibrium distribution of channels through these states should not be altered. However, in Model 3 (asymmetrical trapping scheme) some state transitions are made possible at different membrane potentials by considering that the active receptor complex A_2R^* can shift to either A_2R or A_2R^*B. In order to compensate for the following transition from A_2R^* to A_2R^*B and to observe no changes in the amplitude of next EPC, there should be a significant transition from A_2R^*B to A_2R^* during the rising phase of the endplate current. Good fitting of experimental data was obtained with two modifications: (a) slightly increasing the k_b^-/k_b^+ ratio from 0.008 to 0.01 (for symmetrical and asymmetrical cases, respectively) with increase voltage sensitivity for k_b^-; (b) increasing the α' rate constant value for the transition from the open state A_2R^*B to the closed state A_2RB. With such modifications the asymmetric trapping scheme simulated the interaction of mecamylamine with nAChRs in terms of block relief properties and EPC peak amplitude changes during high frequency nerve stimulation (see Fig. 1Db–Dc; Table 2). Steady state block development (Fig. 1Da) is, however, much faster comparing to block development obtained during experiments (Fig. 1Aa). Adding of the multiple releasing zones and perfusion rate of the experimental chamber slowed down modeled block development (see below). Furthermore, the model closely approximated the voltage and concentration dependence of mecamylamine block as depicted in Fig. 2 in which actual experimental data and modeling results are compared. Another strategy to speed up EPCs decay time was to decrease the β' value. However, in this case it was not possible to decrease the decay time more than on 25% and to simultaneously maintain steady level of EPC amplitude.

Spatio-temporal characteristics of quantal release at whole frog neuromuscular junction

In comparison with the models describing release of a single ACh quanta (Anglister et al. 1994; Friboulet and Thomas 1993; Parnas et al. 1989; Stiles et al. 1996; Wathey et al. 1979) we considered spatio-temporal characteristics of quantal release in the frog neuromuscular junction. Because modeling of the zonal ACh release and drug concentration profile in the recording chamber did not affect shape or behavior of EPCs after full development of mecamylamine block (at steady state), we did not change rate constants of the asymmetrical trapping scheme described in Model 3. Nevertheless, simulated dynamics of

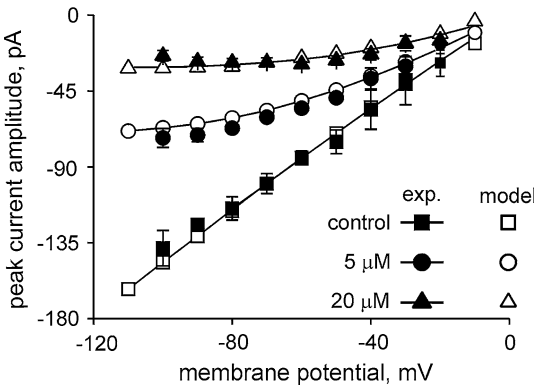

Fig. 2 Asymmetrical trapping scheme reproduces voltage-dependent changes in the amplitude of EPCs in control and after steady state block by different mecamylamine concentrations (5 and 20 μM; for experimentally obtained points $n = 6$ and 8, respectively). Plots show superimposed experimental (*filled symbols*) and computed (*open symbols*) data points

block development was significantly delayed by zonal organization of ACh release and relatively slow rate of chamber perfusion.

There are approximately 300 zones of ACh release on the nerve terminal of the frog neuromuscular junction (Pawson et al. 1998) and not all of them are activated in response to the nerve stimulation. Figure 3a shows a mean number of not activated zones or zones activated once, twice, etc. versus the nerve stimulus number obtained by plotting of equation (5; see Methods). Figure 3b compares development of mecamylamine block for the models with 1 and 300 zones of ACh release (-○- and -□-, respectively). Thus, modeling of the zonal organization of ACh release slowed down calculated time course of mecamylamine block. Further delay in the steady state development of mecamylamine block was observed after consideration of the limited rate of the experimental chamber perfusion. Figure 3b represents calculated changes in the EPCs amplitudes in the model with 300 release zones produced by gradual rise of concentration to 20 μM because of a slow perfusion system (0.35 ml/min; open triangle). In the last case, time profile of mecamylamine block development is compatible with experimentally observed one (Fig. 1Aa).

Discussion

Mecamylamine is a general antagonist of variety nAChRs (Connolly et al. 1992; Papke et al. 2001) acting in competitive (Ascher et al. 1979; Gurney and Rang 1984) or noncompetitive manner (Fieber and Adams 1991; Nooney et al. 1992). Furthermore, it can produce distinct types of block on different cells even within the same tissue (Shen and Horn 1998) and was proposed as a useful tool to characterize the nicotinic receptors from different synapses (Varanda et al. 1985). Moreover, despite that mecamylamine is now rarely used for the treatment of hypertension, recent studies suggest that mecamylamine is very effective for blocking the physiological effects of nicotine and improving abstinence rates in smoking cessation studies (Frishman et al. 2006; Schnoll and Lerman 2006; Shytle et al. 2002). And since mecamylamine can return in the clinical use for smoking cessation it remains important to study mecamylamine action on the whole variety of nAChRs.

Our previous study (Skorinkin et al. 2004) carried out at the frog neuromuscular junction revealed slow in onset, resistant to washout, voltage-dependent reduction of evoked EPCs by different concentrations of mecamylamine. The reduction was always accompanied by significant shortening of EPCs decay time. These findings together with previous studies of mecamylamine action on neuromuscular nAChRs (Albuquerque et al. 1985; Lingle 1983a, b; Varanda et al. 1985) suggest that the action of mecamylamine is mostly due to the direct block of the ionic channel in its open conformation. This is partly confirmed by biochemical studies that showed that mecamylamine does not block [3H]acetylcholine binding to the muscular type of nAChRs (Varanda et al. 1985). Thus, mecamylamine can be identified as "uncompetitive" blocker of nAChRs (Dingledine et al. 1999; Giniatullin et al. 2000; Varanda et al. 1985).

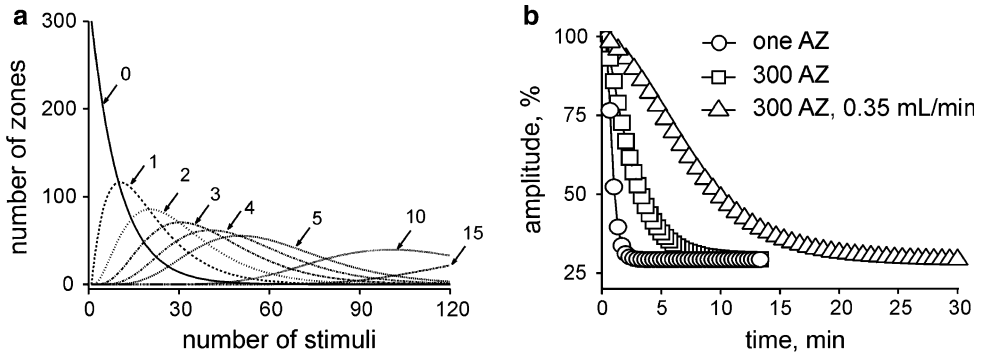

Fig. 3 Zonal organization of acetylcholine release and slow experimental chamber perfusion slow down development of mecamylamine block: simulated experiments. Specific morphological organization of neuromuscular synapses implies that not all releasing zones are activated after single nerve stimulation. **a** *Continuous line* shows that with increasing number of successive stimuli the number of zones that have not been activated falls dramatically. *Broken lines* depict the number of zones that have been activated once, twice, thrice, etc. At 120 stimuli all the zones have been activated at least five times. **b** Plot shows dependence of the simulated mecamylamine block development on the number of activated zones (*circles* for 1; *squares* for 300). For 300 zones probability of a releasing zone activation following nerve stimulation was assumed to be 0.2. *Open triangles* on plot (**b**) show modeled effect of a relatively slow experimental bath perfusion (0.35 ml/min) on the development of mecamylamine block. Note that, by assuming conditions which are close to the experimental (300 AZ; perfusion rate), the simulated dynamic of mecamylamine block development is close to the experimentally obtained one (compare with Fig. 1Aa)

Modeling of receptor activation kinetics is a useful tool to verify experimentally based hypothesis of agonist/antagonist–receptor interaction. This approach has limitations due to currently unknown values of some reaction coefficients that cannot be directly measured. Nevertheless, the fact that simulated responses can match a set of crucial criteria inherent to the action of mecamylamine should prevent unrealistic conclusions. Three most probable kinetic schemes of receptor activation in the presence of mecamylamine have been chosen to be verified: simple open channel block, "symmetrical" trapping block and "asymmetrical" trapping block.

The simple open channel block scheme (even when voltage-dependent interaction of mecamylamine and nAChRs is assumed) shows strong dependence of EPC amplitude on frequency of receptor activation. The high frequency nerve stimulation decreases simulated EPC amplitude after full development of mecamylamine block (Fig. 1Bc). However, our experimental data does not support this tenet (Fig. 1Ac). Multi ion block of nAChRs by mecamylamine was discarded as a model which is a modification of the simple open channel block where unblocking depends only on receptor activation time.

In the early studies (Lambert et al. 1981; Blanpied et al. 1997) "symmetrical" trapping scheme was used, assuming that the nAChRs opening/closing dynamics are the same in control or after antagonist binding inside the channel. Later studies have suggested an "asymmetrical" model based on the changes in the receptor kinetics by antagonist residing within the ionic pore (Dilmore and Johnson 1998; Giniatullin et al. 2000). Since "symmetrical" trapping scheme did not produce steady changes of the EPCs decay time (Fig. 1Ac), "asymmetrical" trapping mechanism was chosen for further analysis. A suitable model describing present data was obtained when a rate constant of transition from the blocked-open state to the blocked-closed state of nAChRs became faster. This observation suggested that, once mecamylamine has bound nAChRs, probability of receptors conversion into inactive state increased despite the presence of ACh. We would like to note that experimentally obtained results were successfully modeled with change of the minimal number of previously defined rate constants (compare with Stiles et al. 1999).

It was shown that desensitization-like phenomenon can only be observed during a sufficiently long period of nerve stimulation, namely 30–60 s with a high frequency (Magleby and Pallota 1981), in particular after acetylcholinesterase inhibition (Giniatullin et al. 1989, 2005). Thus nAChRs desensitization was excluded from the modeling of the mecamylamine effects because of a low frequency nerve stimulation used in our experimental study (Skorinkin et al. 2004).

Block of muscle nAChRs by mecamylamine

Specific organization of the transmitter release in the frog neuromuscular junction was checked to influence agonist/antagonist–receptor interaction. The zonal organization of ACh release implies that not all postsynaptic nAChRs are activated after single nerve stimulation, thus delaying mecamylamine interaction with each single receptor. Our modeling results demonstrate that presence of multiple releasing zones (300; probability of activation after each stimulus was assumed to be 0.2; Pawson et al. 1998) partly explains slow time dynamic of mecamylamine block development. Moreover, simulation of the mecamylamine concentration profile in the experimental chamber after its application results in further delay of the mecamylamine block development to the time range close to the experimentally observed one. Thus slow onset and development of mecamylamine block (comparing to other systems; see Giniatullin et al. 2000) can be caused by morphological peculiarities of the frog neuromuscular junction and experimental conditions.

Functional implications

Neuromuscular transmission in vivo is accompanied by strong muscle depolarization during generation of large amplitude action potentials (Dorrscheidt-Kafer 1981; Knisley et al. 1994; Riemer et al. 1998). Our results predict that the operation of the contracting muscle could be initially preserved by delaying the mecamylamine block through a repeated unblocking mechanism, zonal organization of agonist release and delayed rise of drug concentration. These peculiarities should be taken into account for understanding the pharmacodynamic properties of mecamylamine or other drugs which share the same mechanism of action.

In conclusion, selectivity of action of a receptor blocker toward a particular class of receptors may be determined not only by its affinity for the agonist binding site at certain subunit type combination, but also by its propensity to get trapped inside open channels without preferential affinity for the agonist recognition site. This relief property can be used as a simple test, during ongoing experiments, to establish the presence of a certain type of noncompetitive block by other antagonists as well.

Acknowledgments We thank Prof. A. Nistri and Prof. R. Giniatullin for comments and suggestions during writing of this manuscript. Asya Shaikhutdinova and Andrey Skorinkin would like to thank the Russian Foundation for Basic Research and the Russian government for a Leading Scientific School grant.

References

Albuquerque EX, Deshpande SS, Kawabuchi M, Aracava Y, Idriss M, Rickett DL, Boyne AF (1985) Multiple actions of anticholinesterase agents on chemosensitive synapses: molecular basis for prophylaxis and treatment of organophosphate poisoning. Fundam Appl Toxicol 5:S182–S203

Anglister L, Stiles JR, Salpeter MM (1994) Acetylcholinesterase density and turnover number at frog neuromuscular junctions, with modeling of their role in synaptic function. Neuron 4:783–794

Ascher P, Large WA, Rang HP (1979) Studies on the mechanism of action of acetylcholine antagonists on rat parasympathetic ganglion cells. J Physiol 295:139–170

Baker CT, Bocharov GA, Paul CA, Rihan FA (1998) Modelling and analysis of time-lags in some basic patterns of cell proliferation. J Math Biol 37:341–371

Benveniste M, Mayer ML (1995) Trapping of glutamate and glycine during open channel block of rat hippocampal neuron NMDA receptors by 9-aminoacridine. J Physiol 483:367–384

Blackman JG, Ray C (1964) Actions of mecamylamine, dimecamine, pempidine and their two quaternary metho-salts at the neuromuscular junction. Br J Pharmacol Chemother 22:56–65

Blanpied TA, Boeckman FA, Aizenman E, Johnson JW (1997) Trapping channel block of NMDA-activated responses by amantadine and memantine. J Neurophysiol 77:309–323

Brammar WJ (1996) Nicotinic acetylcholine-gated integral receptors-channels. In: Conley EC, Brammar WJ (eds) The ion channel FactsBook I: extracellular ligand-gated channels. Academic, London, pp 234–292

Chen HS, Lipton SA (1997) Mechanism of memantine block of NMDA-activated channels in rat retinal ganglion cells: uncompetitive antagonism. J Physiol 499:27–46

Chretien JM, Chauvet GA (1998) An algorithmic method for determining the kinetic system of receptor–channel complexes. Math Biosci 147:227–257

Colquhoun D (1998) Binding, gating, affinity and efficacy: the interpretation of structure–activity relationships for agonists and of the effects of mutating receptors. Br J Pharmacol 125:924–947

Connolly J, Boulter J, Heinemann SF (1992) Alpha 4–2 beta 2 and other nicotinic acetylcholine receptor subtypes as targets of psychoactive and addictive drugs. Br J Pharmacol 105:657–666

Corringer PJ, Novere N le, Changeux JP (2000) Nicotinic receptors at the amino acid level. Annu Rev Pharmacol Toxicol 40:431–458

Dilmore JG, Johnson JW (1998) Open channel block and alteration of *N*-methyl-D-aspartic acid receptor gating by an analog of phencyclidine. Biophys J 75:1801–1816

Dingledine R, Borges K, Bowie D, Traynelis SF (1999) The glutamate receptor ion channels. Pharmacol Rev 51:7–61

Dorrscheidt-Kafer M (1981) Comparison of the action of La^{3+} and Ca^{2+} on contraction threshold and other membrane parameters of frog skeletal muscle. J Membr Biol 62:95–103

Fieber LA, Adams DJ (1991) Acetylcholine-evoked currents in cultured neurones dissociated from rat parasympathetic cardiac ganglia. J Physiol 434:215–237

Friboulet A, Thomas D (1993) Reaction–diffusion coupling in a structured system: application to the quantitative simulation of endplate currents. J Theor Biol 160:441–455

Frishman WH, Mitta W, Kupersmith A, Ky T (2006) Nicotine and non-nicotine smoking cessation pharmacotherapies. Cardiol Rev 14:57–73

Giniatullin RA, Khamitov G, Khazipov R, Magazanik LG, Nikolsky EE, Snetkov VA, Vyskocil F (1989) Development of desensitization during repetitive end-plate activity and single end-plate currents in frog muscle. J Physiol 412:113–122

Giniatullin RA, Sokolova EM, Angelantonio S di, Skorinkin A, Talantova MV, Nistri A (2000) Rapid relief of block by mecamylamine of neuronal nicotinic acetylcholine receptors of rat chromaffin cells in vitro: an electrophysiological and modeling study. Mol Pharmacol 58:778–787

Giniatullin R, Nistri A, Yakel JL (2005) Desensitization of nicotinic ACh receptors: shaping cholinergic signaling. Trends Neurosci 28:371–378

Gurney AM, Rang HP (1984) The channel-blocking action of methonium compounds on rat submandibular ganglion cells. Br J Pharmacol 82:623–642

Kalamida D, Poulas K, Avramopoulou V, Fostieri E, Lagoumintzis G, Lazaridis K, Sideri A, Zouridakis M, Tzartos SJ (2007) Muscle and neuronal nicotinic acetylcholine receptors. Structure, function and pathogenicity. FEBS 274:3799–3845

Knisley SB, Smith WM, Ideker RE (1994) Prolongation and shortening of action potentials by electrical shocks in frog ventricular muscle. Am J Physiol 266:H2348–H2358

Lambert JJ, Durant NN, Reynolds LS, Volle RL, Henderson EG (1981) Characterization of end-plate conductance in transected frog muscle: modification by drugs. J Pharmacol Exp Ther 216:62–69

Lingle C (1983a) Blockade of cholinergic channels by chlorisondamine on a crustacean muscle. J Physiol 339:395–417

Lingle C (1983b) Different types of blockade of crustacean acetylcholine-induced currents. J Physiol 339:419–437

Maconochie DJ, Knight DE (1992) Markov modelling of ensemble current relaxations: bovine adrenal nicotinic receptor currents analysed. J Physiol 454:155–182

Magleby KL, Pallotta BS (1981) A study of desensitization of acetylcholine receptors using nerve-released transmitter in the frog. J Physiol 316:225–250

Magleby KL, Stevens CF (1972) The effect of voltage on the time course of end-plate currents. J Physiol 223:151–171

Mathie A, Colquhoun D, Cull-Candy SG (1990) Rectification of currents activated by nicotinic acetylcholine receptors in rat sympathetic ganglion neurones. J Physiol 427:625–655

Naves LA, van der Kloot W (2001) Repetitive nerve stimulation decreases the acetylcholine content of quanta at the frog neuromuscular junction. J Physiol 532:637–647

Neely A, Lingle CJ (1986) Trapping of an open-channel blocker at the frog neuromuscular acetylcholine channel. Biophys J 50:981–986

Nooney JM, Peters JA, Lambert JJ (1992) A patch clamp study of the nicotinic acetylcholine receptor of bovine adrenomedullary chromaffin cells in culture. J Physiol 455:503–527

Papke RL, Sanberg PR, Shytle RD (2001) Analysis of mecamylamine stereoisomers on human nicotinic receptor subtypes. J Pharmacol Exp Ther 297:646–656

Parnas H, Flashner M, Spira ME (1989) Sequential model to describe the nicotinic synaptic current. Biophys J 55:875–884

Pawson PA, Grinnell AD, Wolowske B (1998) Quantitative freeze-fracture analysis of the frog neuromuscular junction synapse—I. Naturally occurring variability in active zone structure. J Neurocytol 27:361–377

Pryaznikov EG, Skorinkin AI, Garaev RS, Giniatullin RA (2002) The mechanism of dimephosphone action on neuromuscular junction. Neirofiziologiya/Neurophysiology 34:361–366

Pryaznikov EG, Skorinkin AI, Garaev RS, Giniatullin RA, Visel AO, Shukina LI (2005) The mechanisms of the action of oxaphospholene derivatives on neuromuscular junction. Bull Exp Biol Med 139:432–435

Riemer TL, Sobie EA, Tung L (1998) Stretch-induced changes in arrhythmogenesis and excitability in experimentally based heart cell models. Am J Physiol 275:H431–H442

Schnoll RA, Lerman C (2006) Current and emerging pharmacotherapies for treating tobacco dependence. Expert Opin Emerg Drugs 11:429–444

Shen WX, Horn JP (1998) Mecamylamine selectively blocks nicotinic receptors on vasomotor sympathetic C neurons. Brain Res 788:118–124

Shytle RD, Penny E, Silver AA, Goldman J, Sanberg PR (2002) Mecamylamine (Inversine): an old antihypertensive with new research directions. J Hum Hypertens 16:453–457

Skorinkin AI (2005) The action of ganglioblocker mecamylamine on the rat's ionotropic muscular cholinoreceptors. Neirofiziologiya/ Neurophysiology 37:217–222

Skorinkin AI, Shaikhutdinova AR (2004) Reconstruction of dynamics of change in the acetylcholine concentration in the synaptic cleft upon signal-quantum signal. Biofizika 49: 872–876

Skorinkin AI, Ostroumov KB, Shaikhutdinova AR, Giniatullin RA (2004) Trapping blockage of muscle nicotinic cholinoreceptors by mecamylamine. Dokl Biol Sci 399:464–466

Stiles JR, Kovyazina IV, Salpeter EE, Salpeter MED MER (1999) The temperature sensitivity of miniature endplate currents is mostly governed by channel gating: evidence from optimized recordings and Monte Carlo simulations. Biophys J 77:1177–1187

Stiles JR, van Helden D, Bartol TM jr, Salpeter EE, Salpeter MM (1996) Miniature endplate current rise times less than 100 microseconds from improved dual recordings can be modeled with passive acetylcholine diffusion from a synaptic vesicle. Proc Natl Acad Sci 93:5747–5752

Varanda WA, Aracava Y, Sherby SM, Vanmeter WG, Eldefrawi ME, Albuquerque EX (1985) The acetylcholine receptor of the neuromuscular junction recognizes mecamylamine as a non-competitive antagonist. Mol Pharmacol 28:128–137

Vargas-Caballero M, Robinson HP (2004) Fast and slow voltage-dependent dynamics of magnesium block in the NMDA receptor: the asymmetric trapping block model. J Neurosci 24:6171–6180

Wathey JC, Nass MM, Lester HA (1979) Numerical reconstruction of the quantal event at nicotinic synapses. Biophys J 27:145–164